



Simplification of Concrete Construction Processes and Rational Use of Eco-friendly Building Materials of BIM Technology in the Perspective of Renewable Energy

Chaowei Wang¹

¹ Sanmenxia Polytechnic
Sanmenxia, Henan (China)
E-mail: 15333989795@163.com

Abstract. As the economy and society continue to grow quickly and as the people's living standards gradually rise, the share of building energy consumption in overall societal energy consumption will continue to rise. Sustainable standards need to be assigned top priority in the building business considering limited resources, impact on the environment, and socioeconomic limits. Additional materials are used to make concrete more sustainable. Several environmental, technological, and financial limitations make the selection of supplemental materials difficult. Building construction costs are capable of being decreased and global emissions of carbon can be reduced through the design optimization of concrete reinforced structures. Based on the above limitations, this paper proposes a new framework in BIM technology. This paper presents an approach for support of decisions that take criteria for sustainability related to social, technical, environmental, and economic aspects when ranking concrete supplemental content. The decision framework comprises the short listing of supplemental materials with technological and cost features based on the OSM, and the following use of ANP to prioritize the materials based on sustainable possibility order. By using the technical properties of every technically sound material utilized as concrete, the current study provides a decision support framework. Based on this, proposing a novel optimization strategy that considers both the structural topology and the optimization of specific components to build high-rise reinforced concrete buildings in a low-carbon and cost-effective manner. This technique first involves determining the optimal structural typology and afterwards optimizes the individual member sizes by using the OCLO algorithm. The suggested method is able to be expanded to optimize different building kinds with comparable issues, increasing the built environment's sustainable development and cost-effectiveness.

Key words. Analytic Network Process, Optimal Scoring Method, Osprey Combined Lyre Bird Optimization, Building Information Modeling, Renewable Energy.

1. Introduction

In the field of AECO, BIM [6] is an innovative technology that possesses the potential to complete change in the buildings planned, designed, constructed, and maintained [21], [22]. However, the AECO sector today accounts for a significant portion of global energy consumption, and as a result, the environmental consequences of its everyday

operations are many [20]. As a result, there is a huge pressure on the AECO field to lower the amounts of emissions that cause pollution and to improve the energy efficiency of its present operations (materials, processes, equipment, buildings) [17], [19]. According to the design phase through the final moments stage, BIM technology plays a critical role in achieving challenging targets [7], [8], [10]. This is for scenarios like facilitating material as well as solution assessments during the design and renovation stages, assessing the inside thermal comfort using BIM models, estimating energy consumption, serving as an environment for visualizing analysis results, and supporting energy certification procedures [9].

Concerning the extent that BIM technology is used to increase building energy efficiency, none has been determined [12]. Hence, a thorough evaluation of the research is required, one that compiles and arranges all of the data pertaining to the present procedures and approaches that allow increased energy efficiency using BIM modeling, as well as any current constraints and potential future advancements [11], [13]. Therefore, the purpose of this article is to assist AECO stakeholders in comprehending all of the methods that BIM might be utilized as a tool to raise energy efficiency levels in the industry [16], [18].

SDO and structural design automation, which both increase the effectiveness of AEC processes, represent the result of the combination of computer technology, contemporary structural engineering, and advancements in construction materials [26]. Furthermore, the structural design field is forced by the application of these computerized methods and instruments to consider important sustainable development aspects into account at the outset of building framework design [25], [27]. These methods are responsible for advancements in computer-aided design and novel frameworks in the area of structural engineering [14], [15]. Because of these revolutionary changes in structural engineering design, structural design is now computerized and optimized and is strongly associated with a number of factors that can be taken into account, such as expenses, credibility, strength, and environmental

sustainability [23], [24]. Thus, this paper proposed a new method for simplification of the concrete construction process and Rational use of Eco friendly building materials of BIM Technology in the perspective of Renewable Energy. The key contribution of this suggested method is summarized below.

Establishing the optimal structural topology via the OCLO algorithm under the consideration of Framework cost, Absolute volume and Linear Inequalities.

Optimizing every member's size by the utilization of the OCLO algorithm under the constraints of embodied carbon, available ranger and material cost.

2. Literature Review

In 2023, RojiniKathiravel *et al.*, [1] examined the economic as well as environmental consequences of various climate conditions in Canadian locations during the lifespan of a structure. Concentrating on the selection of solar, natural gas, and electrical sources for HVAC systems. The research considered three common HVAC systems under six weather situations and looked at 36 scenarios utilizing entire structure life cycle evaluations and energy models. Here, fuzzy-based approaches and BIM were used to reduce uncertainty. Rather than additional life cycle phases differences were mostly caused by the operational, embodied, and transportation phases. Colder regions, such as central Canada, were experiencing greater potential for global warming as well as higher energy demands. When weighing economic and environmental considerations, GSHP was the preferable option due to its reduced emissions, even with greater initial expenditures. However, ASHP works best in temperate climates like Vancouver. Photovoltaic panels increase the viability of HVAC systems in a range of configurations. Legislators, owners, and designers were among the stakeholders in the construction industry who could benefit from the study's insights.

In 2023, Fang Xu and Qiaoran Liu [2] focused on optimizing building energy consumption due to the growing tension between supply and demand for energy. A model for optimizing building energy usage was developed using the concepts of CNNs and BIM. The CNN optimization parameter solution challenge was resolved. Using eQUEST software, a calculation models the tiny size as Revit's three-dimensional design was created for the purpose of simulation. Here, the fundamental analysis variables of the model such as its location, its components' materials, its running schedule and its meteorological data were set as uniform standards. Both the simulation model which was created manually and the model which was automatically created using the enhanced DOE-2 file under the eQUEST software underwent to examine the energy consumption through simulation. In accordance with the pertinent standards, the building's body coefficient was obtained at 0.370 and its window-to-wall ratio in the direction of the east, west, north and south were 0.07, 0.21, 0.30, and 0.16, respectively. Building energy consumption was reported to decrease by 24.53%, increased the natural lighting by 18.98%, and also increased the environmental

pressure hours by 10.57% as compared to the scheme before optimization.

In 2023, PauliusSpudys *et al.*, [3] presented a novel strategy for enhancing current building energy audit procedures through the variation of related data and BIMs. The report outlines the possibility of an evaluation process that makes use of building information models for components audits of energy, which measure the energy consumption of buildings in relation to their envelopes. The possibility of creating novel instruments in this field was discussed, as well as if there was still space for the use of digitalization techniques in doing energy audits. The main outcome of this investigation was the characterization and evaluation of the Industrial Basis Classes model BIM data architecture and its relationships between them, with the goal of using the data gathered to digitize energy inspection methods. The building energy usage evaluation's digitalization impacted by building envelope features and the assessment of energy and economic issues for potential building shell optimization scenarios were covered by the research approach. Therefore, this paper also offers the findings of a real-world assessment that was completed utilizing the newly created instrument and the building envelope alteration feature for a range of environmental and financial factors. Furthermore, the architecture and reasoning behind the tool built are explained. The information needed to perform building energy audits was obtained using this tool.

In 2023, Ahsan Waqar *et al.*, [4] investigated the BIM that promotes efficiency in smaller-scale building projects. With an empirical investigation focused on Perak, Malaysia, the technique includes a thorough literature review as well as a quantitative analysis using SEM and EFA. In small-scale green buildings, the study attempts to evaluate the BIM affects resource utilization, energy consumption, decrease in waste, and cooperative decision-making. The results showed that early-stage optimization of designs, energy consumption analysis, choosing materials, life cycle evaluation, decreased waste, and prefabrication were significantly positively correlated with BIM adoption. This study emphasizes how important it is to include BIM in smaller-scale buildings in order to encourage eco-friendly methods and produce sustainable results. Future studies should look into better ways to integrate BIM and gain more understanding of the cost implications of adopting BIM.

In 2023, Samer El Sayary and Osama Omar [5] developed a new method, which involved using a BIM template created specifically for this purpose to calculate energy use. The template created to calculate the number of solar panels required to build a net-zero energy house was the one with the largest value derived from BIM. The developed BIM prototype was regarded as a helpful tool that can be used by regular, non-specialist users to help achieve a zero-energy home and to spread energy knowledge. It is used as a tool for supporting decisions to incorporate energy simulation into the early stages of zero-energy building design in the field of architecture. Finally, a group of users tested the tool to refine and expand the template's design settings.

3. Building Information Modeling (BIM)

BIM is the process of creating and utilizing a computer software model to simulate the building and running of a facility. The end product is a computerized model of the facility that is intelligent, parametric, and data-rich. It is used to extract and analyze data relevant to different user needs, which helps with decision-making and enhances the facility delivery process [6]. A development in the building business, BIM signifies a move away from computerized drafting and toward a model-based method. Using BIM, a model is created that is not simply a geometric representation but also one that has attributes and properties that project participants can access from anywhere at any time. The creation of a single framework is applied at every stage of a project's life cycle, which is the primary goal of BIM. A BIM model is utilized for a variety of tasks, including facility management, quantity surveys, cost estimation and generating precise shop drawings. It can also be integrated with a time schedule.

In this paper, the ANP technique [28] is used for the selection of supplementary construction material along with sustainable features. Using the OSM, the best technically and financially viable supplementary materials with known technical features are selected for use in the concrete supplementary materials shortlist. The factors taken into account for OSM that have the most impact on blended concrete are surface area, cost, resistance to

chlorides, the amount of CaO and compressive strength. Then integrated ANP method is used to further rank the materials with the highest sustainability scores. The goal is to create a decision support system that evaluates materials to see if they meet the requirements for both technically sound and sustainable performance. The process of formulating an issue identifies pertinent characteristics, standards, and indications that support the problem. Examining the fulfillment of technical, social, economic, and environmental criteria is how the sustainability of the additional concrete material is determined. The selected technical sustainable development indicator for concrete supplementary material takes into consideration the proportionate quantities of the different parts of the concrete, as well as their accessibility, their support for the concrete curing system, the compaction system, the cohesion and consistency of the mix of concrete, and the impact of their extra on the necessities for the durability and strength of the concrete. To achieve social and economic goals, sustainability indicators regarding concrete additional materials include waste material purification, social welfare and security, improved employment, concrete manufacturing expenses, supplemental material expenses for transportation, and lifelong maintenance expenses. The shortlisted supplementary content's relevance weight is determined throughout the selection process in order of sustainability, and rank the additional material. Figure 1 illustrates the suggested ANP-based decision support system and OSM technique for choosing the technically viable sustainable supplemental concrete material.

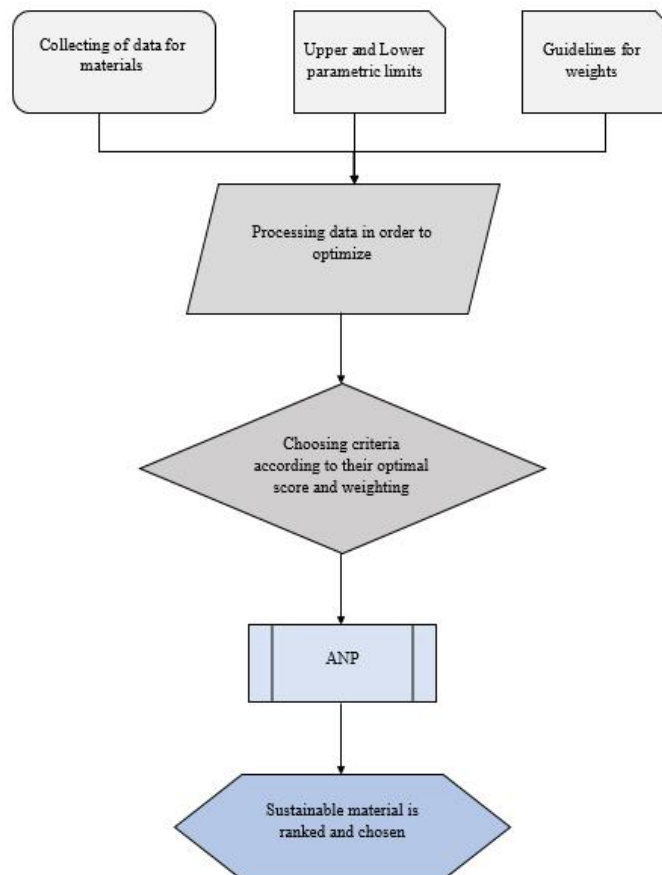


Figure 1. Framework for Choosing Sustainable Supplemental Concrete Material Based on OSM and ANP

A. Selecting Sustainability Assessment Indicators

Technical, social, environmental, and economic variables are taken into consideration while choosing the indicators for the sustainable evaluation. The sustainability of the building materials is also stated for examination. For example, the team was made up of five decision-makers with a combined total of more than five years of work experience. In addition to their own experience, they took into account the opinions of geotechnical experts, environmentalists, building material specialists and government agencies to strengthen the ultimate result of their sustainable materials selection process. The twenty indications that make up the created sustainability evaluation's final list are based on social, environmental, technical and economic criteria, which are explained in section 3.0.

B. OSM for Choosing the Sustainable Supplementary Concrete Material

A system for ranking materials according to a particular purpose is called the OSM [29]. The prospective material, M , represents a single of several possible materials, and an OSM enables the decision-making team to rank it according to the set of assessment standards as K . An additional set of " R " is established for the purpose of making decisions about changing the priority based on the criteria for evaluation. The decision makers have the final say over the guidelines governing the verdict. A range of criteria have been employed to compare the materials; for example, while assessing the material based on criteria Q, R, S, T, U, V , the significance of those criteria remains consistent in that order. The desired weights of the parameters are handled by the other rule; for example, the Q criterion is twice as important as the R criterion, and so on. The cumulative relevance of the combined Q, R , and S criteria in relation to an additional set of criteria, T, U, V , etc., is considered in another rule. "For every assessment criterion $k \in K$, parameters vectors $l = [l_k]$ as well as $u = [u_k]$ specify the lowest and highest bounds on the importance." " $T = [\bar{t}_{mk} \in R] (m \in M, k \in K)$ defines the matrix of understandings of the evaluation criteria, where t_{mk} denotes the evaluation of criteria k for material m ." " $\bar{T} = [\bar{t}_{mk} \in R] (m \in M, k \in K)$ defines a matrix of values that are normalized for converting the evaluation requirements to commensurable units." $Z = [Z_m]$, a dimensionless score vector, is provided by the OSM. By allocating the optimal weights to every criterion $w' = [w'_m]$, it generates a single score for each content. The weights are allocated between 0% and 100% based on the important each criterion is in relation to the others. When one criterion's weight is greater than another, it indicates that the one that was chosen has greater weight when making decisions. The OSM method helps the process of providing

the greatest possible score while remaining on the list of parameters for evaluating the importance of the criteria.

C. Creating the Goal Criteria and Creating a Shortlist of Additional Tangible Material Utilizing OSM

The objective criteria for sustainable performance, which is based on the rating of additional concrete material are determined in this step based on the input of the decision makers [29]. A variety of engineered materials, as well as by-products from the industrial and agricultural sectors, could be used as additional materials for making concrete. The ten most often utilized supplemental materials are nano cement, the supplemental siliceous material's nanoparticles, waste siliceous material (FA, SF, BFS, limestone, rice husk ash,), pozzolanic materials (MN and natural pozzolana), and recycled material (recycled aggregate and waste glass). The OSM method is used to create a shortlist of the supplemental materials according to a scoring rank determined by known technical attributes. The materials selected in the highest scoring sequence are nano cement, siliceous material nanoparticles, FA, BFS, SF, MN, waste glass, limestone, natural pozzolana, recycled aggregate and rice husk ash. Initially, 5 materials with the highest possible ideal score are selected for additional sustainability ranking utilizing the ANP-based technique. It is preferable to use supplemental siliceous material in the form of nanoparticles rather than nano-cement. NPSSM, BFS, FA, MN, as well as SF, are the materials taken into consideration for the sustainability rating.

D. Calculation of Matrix Weight Calculation via ANP for Decision Matrix Normalization

The ANP is created for more complicated issues involving interdependencies between parts. With the ANP technique, the AHP's hierarchical structure starts with a goal and moves down through criteria, sub-criteria, and alternatives to become a network. Through feedback as well as interdependence linkages both inside and between the clusters, the network's all parts, organized into clusters, can be related. The ANP procedure consists of the following four steps:

Step 1: Building the Model

A decision-making problem is stopped in a network where clusters are represented by nodes.

Step 2: Local Priority Vectors and Pairwise Comparisons

To determine the relative weights of the main components and their interdependencies, pairwise comparisons are performed. These pairwise comparisons are applied using the same methodology as the AHP. Next, for every pairwise comparison matrix, the local priority vectors are obtained using the eigenvector approach. To evaluate a pairwise comparison's consistency, a CR is shown. The pairwise comparison is valid if the CR is less than 0.1.

Step 3: Super Matrix Creation

Into the appropriate columns, the local importance vectors are entered for building a super matrix. This partitioned matrix illustrates the connection among the two categories throughout every section. The decomposition of the system into N clusters is shown by G_1, G_2, \dots, G_N . The elements that make up G_l , $1 \leq l \leq N$ are $e_{l1}, e_{l2}, \dots, e_{lnl}$, and nl indicates the total elements there are in the G_l cluster. Eq. (11) shows the super matrix.

$$W' = \begin{matrix} & \begin{matrix} G_1 & & G_2 & & & & G_N \end{matrix} \\ \begin{matrix} G_1 \\ G_2 \\ \vdots \\ G_N \end{matrix} & \begin{bmatrix} e_{11} & \dots & e_{1n1} & e_{21} & \dots & e_{2n2} & e_{N1} & \dots & e_{NnN} \\ W'_{11} & & & W'_{12} & \dots & & & & W'_{1N} \\ W'_{21} & & & W'_{22} & \dots & & & & W'_{2N} \\ \vdots & & & \vdots & \ddots & & & & \vdots \\ W'_{N1} & & & W'_{N2} & & & & & W'_{NN} \end{bmatrix} \end{matrix} \quad (1)$$

With ANP, one has three super matrices. From the pairwise comparison, these local priorities are taken and are included in the unweighted super matrix. To show the weighted super matrix, multiply each element in an unweighted super matrix component by the associated cluster weight matrix, ensuring that the total number in each column equals 1. The eigenvectors of the paired comparison of clusters could provide the cluster weight matrix's column vectors. Multiplying the weighted super matrix through itself yields the limit super matrix. The limit matrix is achieved and the matrix multiplication operation will end when the count of columns for each column equals one another.

Step 4: Final Priorities

The matching columns in the limit super matrices provide the element priorities. To obtain the desirability index, more computations can be performed.

E. Optimization Strategy via OCLO Algorithm

The suggested optimization strategy is explained in this section. The suggested optimization approach begins with modeling the architectural structure of a building, including all of its geometric components, such as beams and walls. Their concrete materials are selected based on the OSM-ANP method. Users must establish the structural system by identifying potential variations in the structural elements, with reference to the building's architectural layout design. Because they are not load-bearing components, certain geometric entities such as partition walls are not included in the structural optimization process. The relationship between various structural parts is then determined for the automated sizing optimization and topological investigation [30]. Two automatic procedures are taken to analyze the structural optimization:

(1) Initially, establish an optimal structural topology via a hybrid optimization algorithm (OCLO) under the constraints of Framework cost, Absolute volume constraints, and Linear Inequality constraints.

(2) Optimizing the size of each member using the OCLO method under the constraints, embodied carbon, Available range and material cost.

Each design must first undergo structural analysis to evaluate the structural performance. Then, each design's member size can be utilized to assess its fitness in terms of available range, material cost, and embodied carbon. The OCLO optimization is done repeatedly to generate new designs up until the optimal solution is identified if, after a predetermined number of generations, the fittest design fails to come to the same value. The architectural model is then updated with the matching structural elements for the best possible outcome. The following sections contain the methodology's specifics.

1) Establishing the Optimal Structural Topology Using OCLO Algorithm

Optimal structural topology refers to the ideal configuration or arrangement of materials within a structure to achieve desired performance criteria while minimizing weight, cost, or other constraints. In this work, to optimize structural topology considering framework cost, absolute volume constraints, and linear inequality constraints by using OCLO algorithm. Specify an absolute volume constraint to ensure that the total volume of material used in the structure does not exceed a certain limit. This constraint helps control the size of the structure. Define linear inequality constraints to incorporate additional requirements such as maximum stress limits, deflection constraints, or geometric constraints. These constraints ensure that the structure satisfies design criteria and performance specifications. Define the objective function that represents the cost of the framework. This function should be minimized to reduce the overall cost of the structure.

a) Objective Function

The objective function of the suggested framework is determined by the minimum of fitness under framework cost, absolute volume and linear Inequality, which is expressed in Eq. (2). W_1 , W_2 , and W_3 are the weight constraints of framework cost, absolute volume and linear Inequality constraints respectively. Eq. (3) shows the calculation of weight constraints, which is defined as the ratio of each constraint to the sum of the constraints.

$$\hat{F} = \min \left(\begin{matrix} W'_1 * \text{framework cost} + W'_2 * (1 - \text{Absolute Volume}) + \\ W'_3 * (1 - \text{Linera Inequality constrain}) \end{matrix} \right) \quad (2)$$

$$W'_i = \frac{\text{Constra ints}(i)}{\sum \text{Constra ints}(i)} \quad (3)$$

b) Initialization

The recommended OCLO approach uses a based on populations metaheuristic method, with Osprey [33] and lyre birds [32] constituting the population. The iteration-

based OCLO algorithm provides adequate solutions for optimization issues by utilizing the group's combined search power in the problem-solving area. In this algorithm, the optimal structural topology is calculated. As a member of the OCLO algorithm, every individual chooses one or more of the decision determinants according to where it is in the problem-solving area. As a result, each individual is represented mathematically as a vector, with a decision variable for every vector element. Organized, OCLO algorithm members make up the algorithm's population, which is represented mathematically by a matrix in accordance with Eq. (4).

Eq. (5) is used to initialize OCLO algorithm members' positions randomly in the problem-solving space. The OCLO algorithm population matrix is represented by T , the i th OCLO algorithm candidate solution is represented by T_i , and the g th dimension in the search space by $T_{i,g}$. The total lyre birds are represented by p , the total decision variables represented by q , and the random number represented by R in the interval $[0,1]$. The lower and upper bounds of the g th decision variable are represented as LB_g and the upper bound is denoted as UB_g .

$$T = \begin{bmatrix} T_1 \\ \vdots \\ T_i \\ \vdots \\ T_p \end{bmatrix}_{p \times q} = \begin{bmatrix} T_{1,1} & \cdots & T_{1,g} & \cdots & T_{1,m} \\ \vdots & \ddots & \vdots & \ddots & \vdots \\ T_{i,1} & \cdots & T_{i,g} & \cdots & T_{i,m} \\ \vdots & \ddots & \vdots & \ddots & \vdots \\ T_{p,1} & \cdots & T_{p,g} & \cdots & T_{p,m} \end{bmatrix}_{p \times q} \quad (4)$$

$$T_{i,d} = LB_d + R \cdot (UB_d - LB_d) \quad (5)$$

c) Mathematical Modeling of OCLO

The suggested OCLO algorithm's architecture updates the population members' positions during each cycle based on a mathematical model. The two phases of the population updating process are (i) escape and (ii) hiding. Eq. (6) simulates the process of a lyrebird's decision-making in the LOA design when it must select between escaping and hiding from threat. During an iteration, the positions of each OCLO member are updated using a single of the first or second phases. The random number R in this case is generated by the interval $[0, 1]$.

Update process for

$$T_i : \begin{cases} \text{Exploration phase 1, } R \leq 0.5 \\ \text{Exploitation phase 2, else} \end{cases} \quad (6)$$

d) Exploration Phase of OCLO Method

Exploration Phase/Escape Strategy using a model of the lyrebird's escape from the threat location to the secure zones, the population member's position is modernized in the search space throughout this phase of OCLO algorithm. The lyrebird's ability to explore numerous parts of the problem-solving area and make large positional changes after moving to a safe place is indicative of OCLO techniques' global search exploration capability. In the

OCLO design, every individual considers the locations of additional population individuals with greater objective function parameters to be secure regions. Therefore, Eq. (7) is used to find the collection of secure regions for each member of the OCLO algorithm. Where, $i = 1, 2, \dots, p$

$$A_i = \{T_s, \widehat{F} < \widehat{F}_i; s \in \{1, 2, \dots, p\}\} \quad (7)$$

The i th lyrebird's list of safe areas is represented by A_i in this case, and the s th row of T matrix is represented by T_s . This row has a higher objective function number (i.e., \widehat{F}_s) compared to the i th OCLO member (i.e., $\widehat{F}_i < \widehat{F}_s$).

It is anticipated in the OCLO design that the lyrebird sometimes makes its way to one of these secure locations. Eq. (8) is used for every OCLO member to determine a new position depending on the lyrebird motion modeling completed in this step. Eq. (9) stands for the simplification of Eq. (8). Here, the lyrebird's chosen safe area is denoted by SA_i , its j th dimension represents $SA_{i,j}$, its new position is established for the i th lyrebird depend on its escape strategy of the proposed OCLO, its j th dimension represents $T_{i,j}^{P1}$ the objective function's value, randomized numbers from the interval $[0, 1]$ are denoted by $R_{i,j}$, and numbers randomly selected as 1 or 2.

$$T_{i,j}^{P1} = T_{i,j} + R_{i,j} \cdot (SA_{i,j} - H_{i,j} \cdot T_{i,j}) \quad (8)$$

$$T_{i,j}^{P1} = T_{i,j} + R_{i,j} \cdot SA_{i,j} - R_{i,j} \cdot H_{i,j} \cdot T_{i,j} \quad (9)$$

In this position, the exploration position of osprey optimization algorithm is induced in this stage. hybrid optimization algorithms offer a versatile and effective approach to structural topology optimization, leveraging the complementary strengths of different optimization techniques to achieve high-quality solutions efficiently. These algorithms play a crucial role in addressing the challenges associated with complex engineering design problems, contributing to the development of innovative and cost-effective structural designs. Eq. (10) shows the position of osprey that moves towards the fish. By simplifying this equation, the current position of the osprey is designed based on the Eqs. (11) to Eq. (15).

$$\widehat{T}_{i,j}^{P1} = \widehat{T}_{i,j} + R'_{i,j} \cdot (F_{i,j} - H'_{i,j} \cdot \widehat{T}_{i,j}) \quad (10)$$

$$\widehat{T}_{i,j}^{P1} = \widehat{T}_{i,j} + R'_{i,j} \cdot F_{i,j} - R'_{i,j} \cdot H'_{i,j} \cdot \widehat{T}_{i,j} \quad (11)$$

$$\widehat{T}_{i,j}^{P1} = \widehat{T}_{i,j} - R'_{i,j} \cdot H'_{i,j} \cdot \widehat{T}_{i,j} + R'_{i,j} \cdot F_{i,j} \quad (12)$$

$$\widehat{T}_{i,j}^{P1} = \widehat{T}_{i,j} (1 - R'_{i,j} \cdot H'_{i,j}) + R'_{i,j} \cdot F_{i,j} \quad (13)$$

$$\widehat{T}_{i,j} (1 - R'_{i,j} \cdot H'_{i,j}) = \widehat{T}_{i,j}^{P1} - R'_{i,j} \cdot F_{i,j} \quad (14)$$

$$\widehat{T}_{i,j} = \frac{\widehat{T}_{i,j}^{P1} - R'_{i,j} \cdot F_{i,j}}{(1 - R'_{i,j} \cdot H'_{i,j})} \quad (15)$$

Substitute Eq. (15) in Eq. (9) for the optimal position in the exploration phase, which is given in Eq. (16). By simplifying the above equation as per Eqns, (17) to Eq. (21) for getting the suitable position.

$$T_{i,j}^{P1} = \left[\frac{\widehat{T}_{i,j}^{P1} - R'_{i,j} \cdot F_{i,j}}{(1 - R'_{i,j} \cdot H'_{i,j})} \right] + R_{i,j} \cdot SA_{i,j} - R_{i,j} \cdot H_{i,j} \cdot \left[\frac{\widehat{T}_{i,j}^{P1} - R'_{i,j} \cdot F_{i,j}}{(1 - R'_{i,j} \cdot H'_{i,j})} \right] \quad (16)$$

$$T_{i,j}^{P1} = \frac{\widehat{T}_{i,j}^{P1}}{(1 - R'_{i,j} \cdot H'_{i,j})} - \frac{R'_{i,j} \cdot F_{i,j}}{(1 - R'_{i,j} \cdot H'_{i,j})} + R_{i,j} \cdot SA_{i,j} - \frac{R_{i,j} \cdot H_{i,j} \cdot \widehat{T}_{i,j}^{P1}}{(1 - R'_{i,j} \cdot H'_{i,j})} + \frac{(R_{i,j})^2 \cdot H_{i,j} \cdot F_{i,j}}{(1 - R'_{i,j} \cdot H'_{i,j})} \quad (17)$$

$$T_{i,j}^{P1} - \frac{\widehat{T}_{i,j}^{P1}}{(1 - R'_{i,j} \cdot H'_{i,j})} + \frac{R_{i,j} \cdot H_{i,j} \cdot \widehat{T}_{i,j}^{P1}}{(1 - R'_{i,j} \cdot H'_{i,j})} = R_{i,j} \cdot SA_{i,j} - \frac{R'_{i,j} \cdot F_{i,j}}{(1 - R'_{i,j} \cdot H'_{i,j})} + \frac{(R_{i,j})^2 \cdot H_{i,j} \cdot F_{i,j}}{(1 - R'_{i,j} \cdot H'_{i,j})} \quad (18)$$

$$T_{i,j}^{P1} \left[1 - \frac{1}{(1 - R'_{i,j} \cdot H'_{i,j})} + \frac{R'_{i,j} \cdot H_{i,j}}{(1 - R'_{i,j} \cdot H'_{i,j})} \right] = R_{i,j} \cdot SA_{i,j} - \frac{R'_{i,j} \cdot F_{i,j}}{(1 - R'_{i,j} \cdot H'_{i,j})} + \frac{(R_{i,j})^2 \cdot H_{i,j} \cdot F_{i,j}}{(1 - R'_{i,j} \cdot H'_{i,j})} \quad (19)$$

$$T_{i,j}^{P1} \left[1 - \frac{1}{(1 - R'_{i,j} \cdot H'_{i,j})} + \frac{R'_{i,j} \cdot H_{i,j}}{(1 - R'_{i,j} \cdot H'_{i,j})} \right] = \left[R_{i,j} \cdot SA_{i,j} - \left[\frac{R'_{i,j} \cdot F_{i,j}}{(1 - R'_{i,j} \cdot H'_{i,j})} (1 + R'_{i,j} \cdot H_{i,j}) \right] \right] \quad (20)$$

$$T_{i,j}^{P1} = \left\{ \frac{\left[R_{i,j} \cdot SA_{i,j} - \left[\frac{R'_{i,j} \cdot F_{i,j}}{(1 - R'_{i,j} \cdot H'_{i,j})} (1 + R'_{i,j} \cdot H_{i,j}) \right] \right]}{\left[1 - \frac{1}{(1 - R'_{i,j} \cdot H'_{i,j})} + \frac{R'_{i,j} \cdot H_{i,j}}{(1 - R'_{i,j} \cdot H'_{i,j})} \right]} \right\} \quad (21)$$

Then, in accordance with Eq. (122), this new location takes the place of the corresponding member's prior position if the current value of the objective function is increased.

$$T_i = \begin{cases} T_i^{P1}, & \widehat{F}_i^{P1} \leq \widehat{F}_i \\ T_i, & \text{else,} \end{cases} \quad (22)$$

e) Exploitation Phase of OCLO Method

During this stage of OCLOA, the population member's position is modified in the search space according to the lyrebird's modeled approach of hiding in its immediate safe area. The lyrebird's position changes somewhat when it moves in little steps to find a good hiding place and accurately scans its surroundings, demonstrating the LOA's potential for use in local searches. Eq. (23) is used in OCLO method design to determine a new position for each OCLO member using the modeling of the lyrebird's migration towards the nearby appropriate region for concealment.

$$T_{i,j}^{P2} = T_{i,j} + (1 - 2R_{i,j}) \cdot \frac{UB_j - LB_j}{t} \quad (23)$$

In this position Eq. (15) of the osprey position is also substituted in Eq. (23) as per Eq. (24). In the exploitation phase, the updated position of OCLO method is simplified in Eq. (25) to Eq. (27).

$$T_{i,j}^{P2} = \left[\frac{\widehat{T}_{i,j}^{P1} - R'_{i,j} \cdot F_{i,j}}{(1 - R'_{i,j} \cdot H'_{i,j})} \right] + (1 - 2R_{i,j}) \cdot \frac{UB_j - LB_j}{t} \quad (24)$$

$$T_{i,j}^{P2} (1 - R'_{i,j} \cdot H'_{i,j}) - \widehat{T}_{i,j}^{P1} = (1 - 2R_{i,j}) \cdot \frac{UB_j - LB_j}{t} - R'_{i,j} \cdot F_{i,j} \quad (25)$$

$$T_{i,j}^{P2} \left[(1 - R'_{i,j} \cdot H'_{i,j}) - 1 \right] = (1 - 2R_{i,j}) \cdot \frac{UB_j - LB_j}{t} - R'_{i,j} \cdot F_{i,j} \quad (26)$$

$$T_{i,j}^{P2} = \frac{\left[(1 - 2R_{i,j}) \cdot \frac{UB_j - LB_j}{t} - R'_{i,j} \cdot F_{i,j} \right]}{\left[(1 - R'_{i,j} \cdot H'_{i,j}) - 1 \right]} \quad (27)$$

Finally, by adding Eq. (21) and Eq. (27) and taking the average of the equation for getting the new updated position as shown in Eq. (28).

$$T_{i,j}^{New} = \frac{\left\{ \frac{\left[R_{i,j} \cdot SA_{i,j} - \left[\frac{R'_{i,j} \cdot F_{i,j}}{(1 - R'_{i,j} \cdot H'_{i,j})} (1 + R'_{i,j} \cdot H_{i,j}) \right] \right]}{\left[1 - \frac{1}{(1 - R'_{i,j} \cdot H'_{i,j})} + \frac{R'_{i,j} \cdot H_{i,j}}{(1 - R'_{i,j} \cdot H'_{i,j})} \right]} \right\} + \frac{\left[(1 - 2R_{i,j}) \cdot \frac{UB_j - LB_j}{t} - R'_{i,j} \cdot F_{i,j} \right]}{\left[(1 - R'_{i,j} \cdot H'_{i,j}) - 1 \right]}}{2} \quad (28)$$

Lastly, Eq. (28) is replaced in Eq. (8) for getting the final new updated position of the OCLO algorithm in the exploration phase. Similarly, the exploitation phase is already mentioned in Eq. (23). This new location replaces the related member's prior position if, as per Eq. (29), it increases the outcome of the objective function.

$$T_i = \begin{cases} T_i^{P2}, & \widehat{F}_i^{P2} \leq \widehat{F}_i \\ T_i, & \text{else,} \end{cases} \quad (29)$$

The lyrebird's dimension is represented by $T_{i,j}^{P2}$, its objective function value is \widehat{F}_i^{P2} , random values from the interval $[0, 1]$, and the iteration counter is t . In this case, T_i^{P2} represents the new position determined for the lyrebird depending on the concealing approach of the suggested OCLO algorithm.

f) Flowchart of OCLOA and Repetition Process

The first OCLOA iteration is finished when all lyrebird positions are updated. After that, the algorithm moves on to the following iteration, and until the last iteration, the OCLOA population is updated using Eq. (6) to Eq. (29). The optimal candidate solution is updated and saved after every iteration.

The optimal candidate solution that was saved throughout the algorithm's iterations is reported as the problem's solution following the entire program of OCLO algorithm. In Figure 2, the OCLO algorithm implementation processes are given as a flowchart. The work process is as follows, according to the OCLO flowchart: initially, the algorithm's input is filled with problem information on the objective function, constraints, and decision variables. The population size and the number of iterations needed to solve the given problem are then determined. The algorithm's initial population is generated at random in the first phase, and it is then evaluated using the problem's objective function.

The algorithm starts its first iteration after the initialization phase. Subsequently, the initial lyrebird's position within the problem-solving space is updated. When faced with danger, the lyre bird has two options, as outlined in OCLO modeling: (i) escape; (ii) hide. Based on Eq. (6), it is assumed in OCLOA design that each lyrebird randomly chooses one of these two tactics with equal likelihood. Eq. (7) to Eq. (22) are used to update the position in the problem-solving space if it decides to use the escape route. Eq. (23) to Eq. (29) are used to update the lyrebird's position in the problem-solving space if it decides to hide. Thus far, there has been a successful update to the position of the population member.

Then, using the same procedure as for updating the first structural arrangement, the positions of additional structural members arrangement are updated in the problem-solving area. At this point, the algorithm's first iteration is finished, with every position in the problem-solving space updated. Up until this iteration is stored, the best candidate solution is found by comparing the evaluated values for the objective function. The algorithm then moves on to the following iteration, where updating the problem-solving space is done in a manner similar to that described in the previous iteration and continues until the algorithm reaches its final iteration.

The optimal solution found during algorithm iterations is added to the output as a solution to the specified problem once all algorithm iterations have been completed. This marks the successful conclusion of the algorithm's implementation.

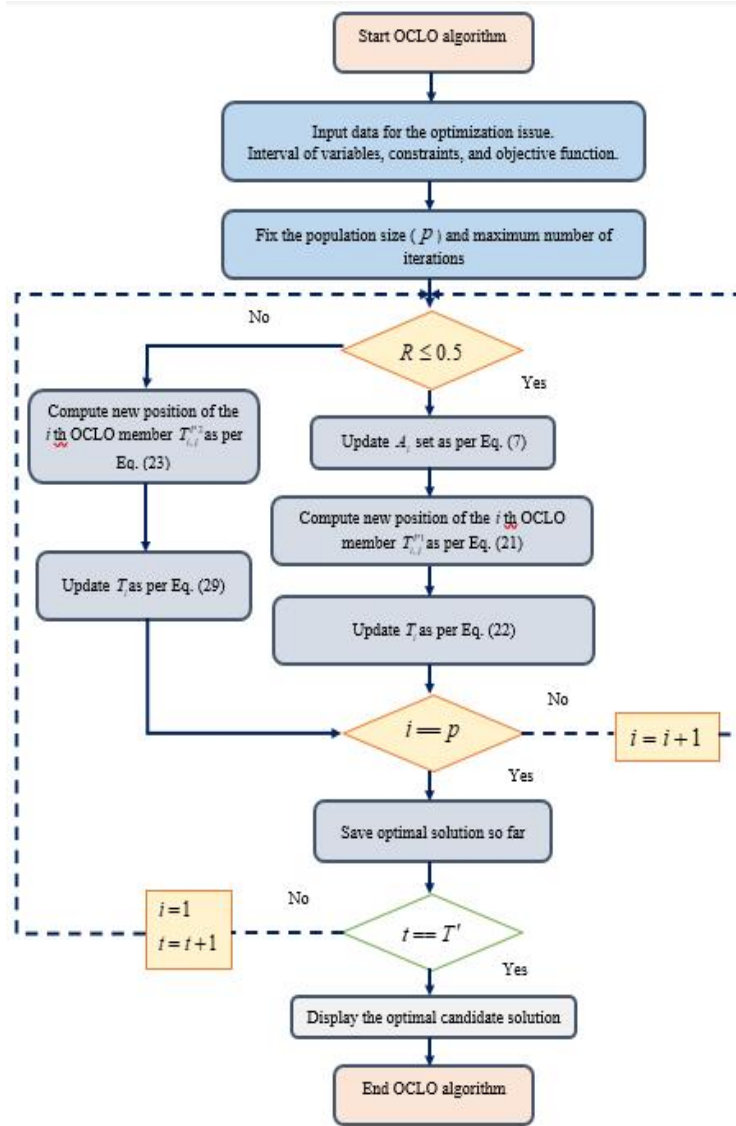


Figure 2. Flowchart of OCLO Algorithm

2) Optimizing the Size of Each Member via OCLO Algorithm

Optimizing the size of each concrete member in a structural system involves finding the dimensions that minimize material usage while satisfying design constraints such as strength, stiffness, and serviceability requirements [31]. In this proposed work, the OCLO algorithm is used for optimizing size under the constraints of embodied carbon, available range and material cost.

The objective function of the proposed model is determined by the minimum of fitness under framework cost, absolute volume and linear Inequality, which is expressed in Eq. (30). W_1' , W_2' , and W_3' are the weight constraints of embedded carbon, available energy and material cost constrains respectively. The calculation of weight constraints, is defined as the ratio of each constraint to the sum of the constraints as given in Eq. (3).

$$\hat{F} = \min \left(\begin{array}{l} W_1' * \text{embedded carbon} + W_2' * (1 - \text{Available range}) + \\ W_3' * \text{material cost} \end{array} \right) \quad (30)$$

Optimizing the size of each structural member while considering embedded carbon constraints, available range, and material cost constraints involves integrating sustainability considerations, practical limitations, and economic factors into the optimization process.

According to the embedded carbon constraints, calculate the embedded carbon footprint associated with the production and use of different concrete member sizes. Consider factors such as material extraction, transportation, manufacturing, and end-of-life disposal. Define a maximum allowable carbon footprint or establish carbon reduction targets based on sustainability goals and regulatory requirements. Incorporate embedded carbon emissions as an additional constraint in the optimization problem formulation. This constraint ensures that the optimized design minimizes the environmental impact associated with concrete usage.

From the available range constraints, Identify the available range of sizes for each structural member based on manufacturing capabilities, construction practices, and design specifications. Define constraints on member

dimensions to ensure that the optimized design falls within the feasible range of sizes. These constraints prevent the algorithm from exploring infeasible solutions that cannot be practically realized.

Finally, Estimate the material costs associated with different concrete member sizes, including material procurement, fabrication, installation, and maintenance expenses. Define a budget or cost target for the project based on economic considerations and budgetary constraints. Integrate material cost constraints into the optimization problem formulation to ensure that the optimized design remains within the budgetary limits while minimizing material usage.

Based on these constraints, the dimension of the structural member is optimized by using the OCLO algorithm, which procedure is already mentioned in Eq. (4) to Eq. (29).

4. Results and Discussion

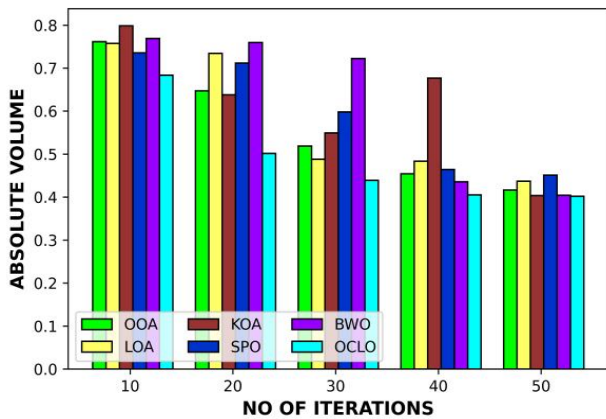
A. Simulation Procedure

This proposed methodology was implemented in PYTHON, and the version utilized was "Python 3.7". The processor utilized was the "11th Gen Intel(R) Core(TM) i5-1135G7 @ 2.40GHz 2.42 GHz". The installed RAM size was "16.0 GB". We have compared our OCLO algorithm's implementation outcomes over other models like OOA, KOA, BWO, LOA and SPO models for diverse iterations that are briefed below.

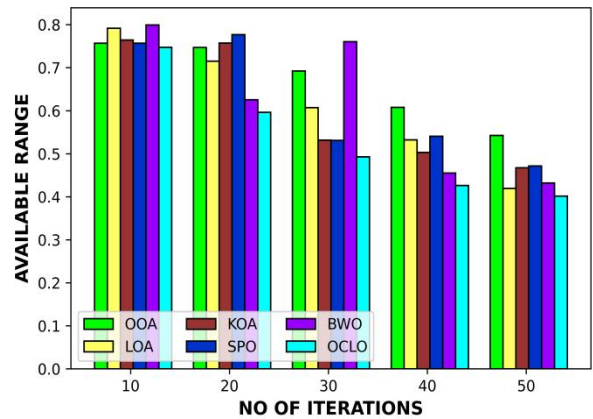
B. Analysis of Absolute Volume, Available Range and Ratio Constraints

We have analyzed the absolute volume, available range and ratio constraints of OCLO algorithm for 0-50 iterations, and the outcomes are displayed in Figure 3. A condition was represented by the absolute volume formula, which states that the total volume of the concrete's components should correspond to the 1 cubic meter of concrete's volume. As per this condition, an effective model should have lower absolute volume, available range and ratio constraints. As seen in Figure 3 (a), minimal absolute volume was attained by our OCLO algorithm, meanwhile, OOA, KOA, BWO, LOA and SPO models attained 0.76, 0.79, 0.77, 0.75 and 0.71 during the 10th iteration. Furthermore, at 40-th iteration, OOA LOA, KOA, SPO, and BWO models attained the ratings of 0.45, 0.48, 0.68, 0.46, and 0.44, while OCLO algorithm attained only 0.4.

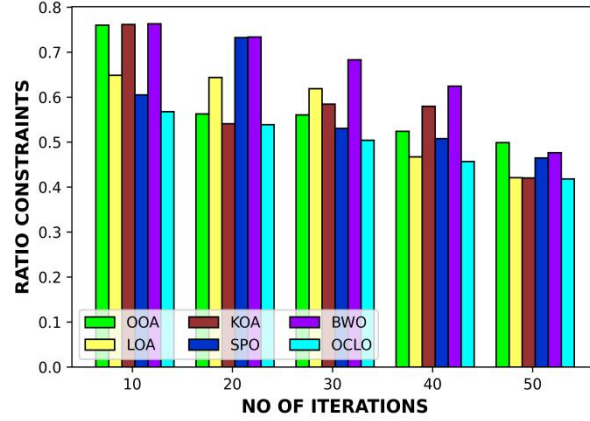
Similarly, we have analyzed the OCLO algorithm's ratio and available range constraints for 0-50 iterations and outcomes are seen in Figure 3 (b) and Figure 3 (c). Mainly, in our OCLO algorithm, search space reduction and search space acceleration are contributed by this ratio constraint. In addition, the concrete mix design's experience and regulation are reflected by the available range constraint. A better approach should obtain a lower ratio and available range constraints. As per this statement, our OCLO algorithm attained the available range values of 0.74, 0.59, 0.49, 0.42 and 0.41 for 10-50 iterations, meanwhile, other LOA, KOA, SPO, and BWO models attained higher values than that. As seen in Figure 3 (c), not only in the case of available range constraints, for ratio constraints also our OCLO algorithm attained the lowest ratings which are 0.57, 0.55, 0.53, 0.49 and 0.47 for 10-50 iterations.



Absolute Volume



Available Range



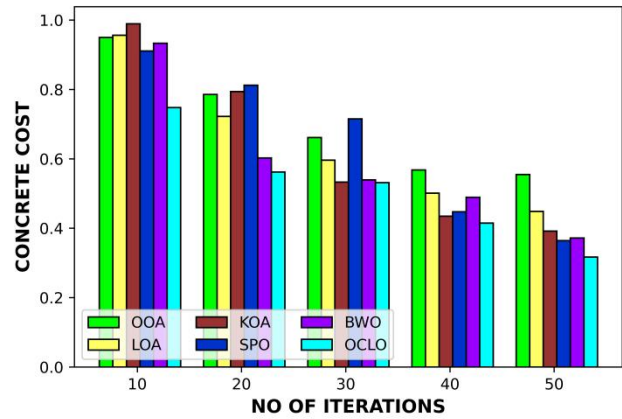
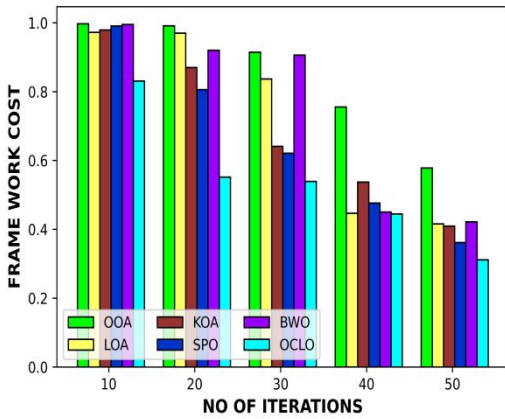
Ratio Constraints

Figure 3. Analysis of Proposed OCLO Algorithm's Constraints over Other Models

C. Analysis of Framework and Material Costs

An analysis was conducted on our OCLO algorithm's framework and material costs, and their outcomes are compared over LOA, KOA, SPO, and BWO models. That can be seen in Figure 4. Generally, expenses correlated with our OCLO algorithm were named as the framework cost. As seen in Figure 4 (a), minimal framework cost rating i.e., 0.81 was attained by our OCLO algorithm, while OOA, KOA, BWO, LOA and SPO models attained the ratings of 1, 0.86, 0.87, 0.88 and 1 at 10th iteration.

Similarly, for 20, 30, 40 and 50th iterations also our OCLO algorithm attained ratings of 0.46, 0.45, 0.43 and 0.36, which are lower than OOA, LOA, KOA, SPO, and BWO models. Moreover, Figure 4 (b) depicts that our OCLO algorithm attained the concrete cost rating of 0.74, 0.58, 0.56, 0.45 and 0.37, for 10-50 iterations, while other LOA, KOA, SPO, and BWO models attained the higher values than that. From these outcomes, it was proven that our OCLO algorithm can effectively explore the design space and lower the concrete cost without compromising structural safety and integrity.



Framework Cost

Concrete Cost

Figure 4. Analysis of Proposed OCLO Algorithm's Framework and Concrete Cost over Other Models

D. Convergence Analysis

Convergence analysis was conducted on our OCLO algorithm for 0-50 iterations and the outcomes were compared over LOA, KOA, SPO, and BWO models, that was shown in Figure 5. From 0-10th iteration, our OCLO algorithm converges to 0.942 from 0.9451, while other

OOA, LOA, KOA, SPO, and BWO model converges to > 0.943. At 20-40th iteration, stable convergence rate of 0.9398 was by our OCLO algorithm while other models attained higher ratings. Finally, after 40th iteration, our OCLO algorithm's convergence reaches 0.935, while other models have higher convergence. These outcomes showed the OCLO algorithm's superior performance.

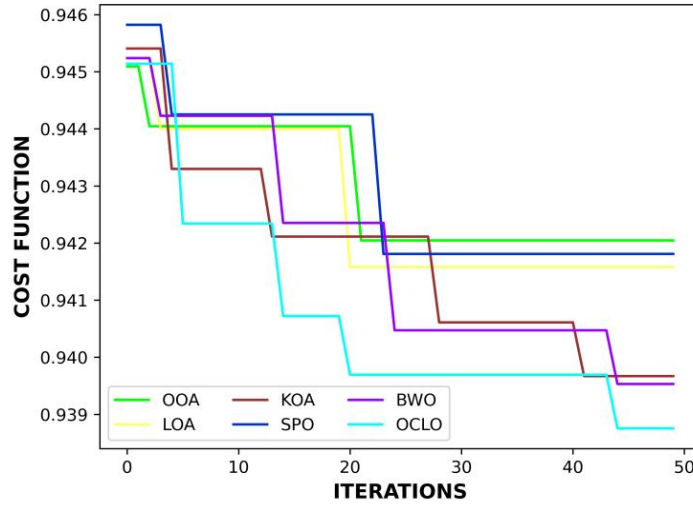
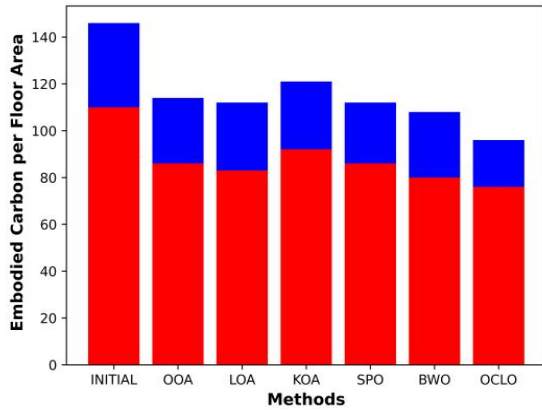


Figure 5. Proposed OCLO Algorithm's Convergence Analysis Comparison over Other Models

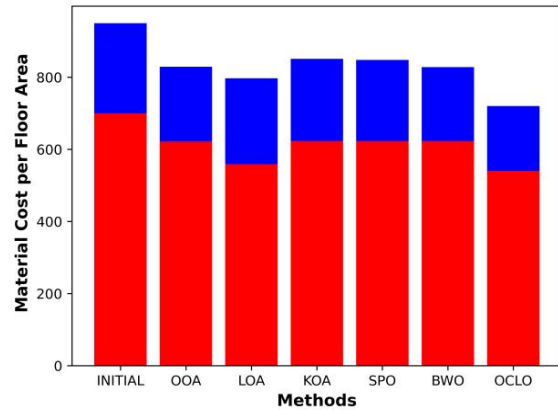
E. Analysis of Embodied Carbon and Material Cost

The embodied carbon along with material cost/floor area analysis comparison has been provided in Figure 6. Initially, embodied carbon and material cost/floor area are 880 and 145. However, after using our OCLO algorithm, the model has embodied carbon and material cost/floor area ratings of 780 and 100. The material cost and carbon

emission are disaggregated into diverse kinds of building members. Similarly, embodied carbon and material cost/floor area of the designs which use other OOA, LOA, KOA, SPO, and BWO models are also compared with our OCLO algorithm which can be seen in Figure 5. From these outcomes, it was proven that cost efficiency along with carbon performance was enhanced by our OCLO algorithm.



(a) Embodied Carbon/Per Floor Area



(b) Material Cost/Per Floor Area

Figure 6. Analysis of OCLO Algorithm's Embodied Carbon and Material Cost over Other Models

F. Statistical Analysis

Statistical analysis was conducted in terms of an error in our OCLO algorithm and the outcomes were compared over other models such as OOA, LOA, KOA, SPO, and BWO, which is given in Table 1. Initially, our OCLO algorithm attained the standard deviation, mean, median, min and max values of 0.002, 0.941, 0.940, 0.939 and

0.945, while BWO attained 0.002, 0.942, 0.940, 0.940 and 0.945, this highest ratings indicates the highest error ratings. Moreover, SPO attained the deviation, mean, median, min and max values of 0.001, 0.943, 0.942, 0.942 and 0.946, that BES has a slightly higher error rating than other our OCLO algorithm. This indicates our OCLO algorithm provides better performance with less error.

Table 1. Statistical Analysis of OCLO Algorithm's Performance over Other Models

No.	Method	Standard Deviation	Mean	Median	Max	Min
0	OOA	0.001	0.943	0.942	0.945	0.942
1	LOA	0.001	0.943	0.942	0.945	0.942
2	KOA	0.002	0.942	0.942	0.945	0.940
3	SPO	0.001	0.943	0.942	0.946	0.942
4	BWO	0.002	0.942	0.940	0.945	0.940

5	OCLO	0.002	0.941	0.940	0.945	0.939
---	------	-------	-------	-------	-------	-------

5. Conclusion

This study offers a method for evaluating concrete supplemental content that considers sustainability in terms of technological, environmental, social, and economic factors. The decision framework consists of using the OSM to shortlist additional resources with cost and technological attributes, and then using ANP to rank the materials according to sustainable possibility order. Based on the technical characteristics of all technically sound materials used as concrete, this investigation offered a structure for decision support. Based on this, develop a novel optimization technique that balances the optimization of individual components with the structural topology to build high-rise reinforced concrete buildings in a way that is both economical and low-carbon. Using the OCLO algorithm, this technique optimizes individual member sizes after identifying the best structural typology. The proposed approach was able to be extended to optimize various building types with similar problems, improving the cost-effectiveness and sustainable growth of the built environment.

References

- [1] R. Kathiravel, S. Zhu, and H. Feng, "LCA of net-zero energy residential buildings with different HVAC systems across Canadian climates: A BIM-based fuzzy approach," *Energy and Buildings*, vol. 306, p. 113905, Mar. 2024, doi: 10.1016/j.enbuild.2024.113905.
- [2] F. Xu and Q. Liu, "Building energy consumption optimization method based on convolutional neural network and BIM," *Alexandria Engineering Journal*, vol. 77, pp. 407-417, Aug. 2023, doi: 10.1016/j.aej.2023.06.084.
- [3] P. Spudys, A. Jurelionis, and P. Fokaidis, "Conducting smart energy audits of buildings with the use of building information modelling," *Energy and Buildings*, vol. 285, Apr. 2023, doi: 10.1016/j.enbuild.2023.112884.
- [4] A. Waqar, I. Othman, N. Saad, M. Azab, and A. M. Khan, "BIM in green building: Enhancing sustainability in the small construction project," *Cleaner Environmental Systems*, vol. 11, Dec. 2023, doi: 10.1016/j.cesys.2023.100149.
- [5] S. El Sayary and O. Omar, "Designing a BIM energy-consumption template to calculate and achieve a net-zero-energy house," *Solar Energy*, vol. 216, 1 Mar. 2021, pp. 315-320, doi: 10.1016/j.solener.2021.01.003.
- [6] G. Liu, G. Liu, and W. Jiang, "Modeling and calculation of shear capacity of prestressed high strength concrete beams with web reinforcement based on BIM," *Ain Shams Engineering Journal*, vol. 15, no. 1, Jan. 2024, doi: 10.1016/j.asej.2023.102360.
- [7] C. Shen, B. Jiang, and L. Yue, "LSTM combined with BIM technology in the management of small and medium-sized span highway concrete beam bridges," *Results in Engineering*, vol. 20, Dec. 2023, doi: 10.1016/j.rineng.2023.101539.
- [8] G. Yilmaz, A. Akcamete, and O. Demirors, "BIM-CAREM: Assessing the BIM capabilities of design, construction and facilities management processes in the construction industry," *Computers in Industry*, vol. 147, May 2023, doi: 10.1016/j.compind.2023.103861.
- [9] M. Johansson and M. Roup, "Real-world applications of BIM and immersive VR in construction," *Automation in Construction*, vol. 158, Feb. 2024, doi: 10.1016/j.autcon.2023.105233.
- [10] J. Zhang, J. Li, B. Liu, H. Li, and W. Yang, "The design and application of BIM + refined management and control platform for the Jingxiong railway bridge," *High-speed Railway*, vol. 1, no. 3, Sep. 2023, pp. 211-218, doi: 10.1016/j.hspr.2023.07.001.
- [11] H. Xu, R. Chang, N. Dong, J. Zuo, and R. J. Webber, "Interaction mechanism of BIM application barriers in prefabricated construction and driving strategies from stakeholders' perspectives," *Ain Shams Engineering Journal*, vol. 14, no. 1, Feb. 2023, doi: 10.1016/j.asej.2022.101821.
- [12] C. Zhang, F. Wang, Y. Zou, J. Dimyadi, B. H. W. Guo, and L. Hou, "Automated UAV image-to-BIM registration for building façade inspection using improved generalised Hough transform," *Automation in Construction*, vol. 153, Sep. 2023, doi: 10.1016/j.autcon.2023.104957.
- [13] L. D'Angelo, M. Hajdukiewicz, F. Seri, and M. M. Keane, "A novel BIM-based process workflow for building retrofit," *Journal of Building Engineering*, vol. 50, Jun. 2022, doi: 10.1016/j.jobe.2022.104163.
- [14] Y. Wang, H. Lu, Y. Wang, Z. Yang, Q. Wang, and H. Zhang, "A hybrid building information modeling and collaboration platform for automation system in smart construction," *Alexandria Engineering Journal*, vol. 88, Feb. 2024, pp. 80-90, doi: 10.1016/j.aej.2024.01.013.
- [15] A. Meoni, F. Vittori, C. Piselli, A. D'Alessandro, A. L. Pisello, and F. Ubertini, "Integration of structural performance and human-centric comfort monitoring in historical building information modeling," *Automation in Construction*, vol. 138, Jun. 2022, doi: 10.1016/j.autcon.2022.104220.
- [16] G. Chen, Z. Yan, J. Chen, and Q. Li, "Building information modeling (BIM) outsourcing decisions of contractors in the construction industry: Constructing and validating a conceptual model," *Developments in the Built Environment*, vol. 12, Dec. 2022, doi: 10.1016/j.dibe.2022.100090.
- [17] F. Minelli, I. Ciriello, F. Minichiello, and D. D'Agostino, "From net zero energy buildings to an energy sharing model - The role of NZEBs in renewable energy communities," *Renewable Energy*, Feb. 2024, doi: 10.1016/j.renene.2024.120110.
- [18] J. E. Latupeirissa and H. Arrang, "Sustainability factors of building information modeling (BIM) for a successful construction project management life cycle in Indonesia," *Journal of Building Pathology and Rehabilitation*, vol. 9, no. 26, 2024, doi: 10.1007/s41024-023-00376-1.
- [19] M. Alzara, Y. A. Attia, S. Y. Mahfouz, A. M. Yosri, and A. Ehab, "Building a genetic algorithm-based and BIM-based 5D time and cost optimization model," *IEEE Access*, vol. 11, pp. 122502-122515, 2023, doi: 10.1109/ACCESS.2023.3317137.
- [20] Z. Xiang, G. Ou, and A. Rashidi, "An integrated framework for BIM development of concrete buildings containing both surface elements and rebar," *IEEE Access*, vol. 11, pp. 15271-15283, 2023, doi: 10.1109/ACCESS.2023.3244689.
- [21] J. Xue, X. Hou, and Y. Zeng, "Rough registration of BIM element projection for construction progress tracking," *IEEE Access*, vol. 10, pp. 8305-8316, 2022, doi: 10.1109/ACCESS.2022.3144150.
- [22] J. Sresakoolchai and S. Kaewunruen, "Integration of building information modeling and machine learning for railway defect localization," *IEEE Access*, vol. 9, pp. 166039-166047, 2021, doi: 10.1109/ACCESS.2021.3135451.
- [23] Y. Ni, B. Sun, and Y. Wang, "Blockchain-based BIM digital project management mechanism research," *IEEE*

- Access*, vol. 9, pp. 161342-161351, 2021, doi: 10.1109/ACCESS.2021.3130270.
- [24] Y. Xiang, K. Liu, T. Su, J. Li, S. Ouyang, S. S. Mao, and M. Geimer, "An extension of BIM using AI: A multi working-machines pathfinding solution," *IEEE Access*, vol. 9, pp. 124583-124599, 2021, doi: 10.1109/ACCESS.2021.3110937.
- [25] Y. Feng, J. Wang, H. Fan, and Y. Hu, "A BIM-based coordination support system for emergency response," *IEEE Access*, vol. 9, pp. 68814-68825, 2021, doi: 10.1109/ACCESS.2021.3077237.
- [26] C. Zhang, A. X. Zhu, L. Zhou, M. Che, and T. Qiu, "Constraints for improving information integrity in information conversion from CAD building drawings to BIM model," *IEEE Access*, vol. 8, pp. 81190-81208, 2020, doi: 10.1109/ACCESS.2020.2991200.
- [27] F. Wang, X. Xu, M. Chen, J. Nzige, and F. Chong, "Simulation research on fire evacuation of large public buildings based on building information modeling," *Complex System Modeling and Simulation*, vol. 1, no. 2, pp. 122-130, Jun. 2021, doi: 10.23919/CSMS.2021.0012.
- [28] S. Mahmoudkelaye, K. T. Azari, M. Pourvaziri, and E. Asadian, "Sustainable material selection for building enclosure through ANP method," *Case Studies in Construction Materials*, vol. 9, 2018, doi: 10.1016/j.cscm.2018.e00200.
- [29] M. Ahmed, M. N. Qureshi, J. Mallick, and N. B. Kahla, "Selection of sustainable supplementary concrete materials using OSM-AHP-TOPSIS approach," *Hindawi, Advances in Materials Science and Engineering*, vol. 2019, no. 1, 2019, doi: 10.1155/2019/2850480.
- [30] V. J. Gan, C. L. Wong, K. T. Tse, J. C. Cheng, I. M. Lo, and C. M. Chan, "Parametric modelling and evolutionary optimization for cost-optimal and low-carbon design of high-rise reinforced concrete buildings," *Advanced Engineering Informatics*, vol. 42, 2019, doi: 10.1016/j.aei.2019.100962.
- [31] H. Dehnavipour, M. Mehrabani, A. Fakhriyat, and A. J. Gałczyńska, "Optimization-based design of 3D reinforced concrete structures," *Journal of Soft Computing in Civil Engineering*, vol. 3, pp. 95-106, 2019, doi: 10.22115/SCCE.2020.211509.1145.
- [32] M. Dehghani, G. Bektemyssova, Z. Montazeri, G. Shaikemelev, O. P. Malik, and G. Dhiman, "Lyrebird optimization algorithm: A new bio-inspired metaheuristic algorithm for solving optimization problems," *Biomimetics*, vol. 8, no. 6, 2023, doi: 10.3390/biomimetics8060507.
- [33] M. Dehghani and P. Trojovský, "Osprey optimization algorithm: A new bio-inspired metaheuristic algorithm for solving engineering optimization problems," *Frontiers in Mechanical Engineering*, vol. 8, 2023, doi: 10.3389/fmech.2022.1126450.

Appendix

Table 2. Nomenclature

Abbreviation	Description
AECO	Architecture, Engineering, Construction, and Operations
AHP	Analytic Hierarchy Process
ANP	Analytic Network Process
ASHP	Air Source Heat Pumps
BFS	Blast Furnace Slag
BIM	Building Information Modeling
BWO	Black Widow Optimization
CNN	Conventional Neural Network
CR	Consistency Ratio
EFA	Exploratory Factor Analysis
FA	Fly Ash
GSHP	Ground Source Heat Pump
HVAC	Heating, Ventilation and Air Conditioning
KOA	Kookaburra Optimization Algorithm
LOA	Lyrebird Optimization Algorithm
MN	Metakaolin
NPSSM	Nanoparticles of Supplemental Siliceous Material
OCLO	Osprey Combined Lyre Bird Optimization
OSM	Optimal Scoring Method
OOA	Osprey Optimization Algorithm
SPO	Sandpiper Optimization
SDO	Structural Design Optimization
SEM	Structural Equation Modeling
SF	Silica Fume